



**Fermi National Accelerator Laboratory**

**FERMILAB-Pub-97/245-E**

**E771**

**Differential Cross Sections of  $J/\psi$   
and  $\psi'$  in 800 GeV/c p-Si Interactions**

T. Alexopoulos et al.  
The E771 Collaboration

*Fermi National Accelerator Laboratory  
P.O. Box 500, Batavia, Illinois 60510*

July 1997

Submitted to *Physical Review D*

## **Disclaimer**

*This report was prepared as an account of work sponsored by an agency of the United States Government. Neither the United States Government nor any agency thereof, nor any of their employees, makes any warranty, expressed or implied, or assumes any legal liability or responsibility for the accuracy, completeness, or usefulness of any information, apparatus, product, or process disclosed, or represents that its use would not infringe privately owned rights. Reference herein to any specific commercial product, process, or service by trade name, trademark, manufacturer, or otherwise, does not necessarily constitute or imply its endorsement, recommendation, or favoring by the United States Government or any agency thereof. The views and opinions of authors expressed herein do not necessarily state or reflect those of the United States Government or any agency thereof.*

## **Distribution**

*Approved for public release; further dissemination unlimited.*

# Differential cross sections of $J/\psi$ and $\psi'$ in 800 GeV/c p-Si interactions

T. Alexopoulos<sup>1</sup>, L. Antoniazzi<sup>2</sup>, M. Arenton<sup>3</sup>, H.C. Ballagh<sup>4</sup>, H. Bingham<sup>4†</sup>,  
A. Blankman<sup>5</sup>, M. Block<sup>6</sup>, A. Boden<sup>7</sup>, G. Bonomi<sup>2</sup>, Z.L. Cao<sup>3</sup>, T.Y. Chen<sup>8</sup>, K. Clark<sup>9</sup>,  
D. Cline<sup>7</sup>, S. Conetti<sup>3</sup>, M. Cooper<sup>10</sup>, G. Corti<sup>3</sup>, B. Cox<sup>3</sup>, P. Creti<sup>11</sup>, C. Dukes<sup>3</sup>,  
C. Durandet<sup>1</sup>, V. Elia<sup>11</sup>, A.R. Erwin<sup>1</sup>, L. Fortney<sup>12</sup>, V. Golovatyuk<sup>11</sup>, E. Gorini<sup>11</sup>,  
F. Grancagnolo<sup>11</sup>, K. Hagan-Ingram<sup>3</sup>, M. Haire<sup>13</sup>, P. Hanlet<sup>3</sup>, M. He<sup>14</sup>, G. Introzzi<sup>2</sup>,  
M. Jenkins<sup>9</sup>, D. Judd<sup>13</sup>, W. Kononenko<sup>5</sup>, W. Kowald<sup>12</sup>, K. Lau<sup>15</sup>, A. Ledovskoy<sup>3</sup>,  
G. Liguori<sup>2</sup>, J. Lys<sup>4</sup>, P.O. Mazur<sup>16</sup>, A. McManus<sup>3</sup>, S. Misawa<sup>4</sup>, G.H. Mo<sup>15</sup>, C.T. Murphy<sup>16</sup>,  
K. Nelson<sup>3</sup>, M. Panareo<sup>11</sup>, V. Pogosian<sup>3</sup>, S. Ramachandran<sup>7</sup>, J. Rhoades<sup>7</sup>, W. Selove<sup>5</sup>,  
R.P. Smith<sup>16</sup>, L. Spiegel<sup>16</sup>, J.G. Sun<sup>3</sup>, S. Tokar<sup>17</sup>, P. Torre<sup>2</sup>, J. Trischuk<sup>18</sup>, L. Turnbull<sup>13</sup>,  
D.E. Wagoner<sup>13</sup>, C.R. Wang<sup>14</sup>, C. Wei<sup>12</sup>, W. Yang<sup>16</sup>, N. Yao<sup>8</sup>, N.J. Zhang<sup>14</sup>, and  
B.T. Zou<sup>12</sup>

<sup>1</sup> *University of Wisconsin, Madison, Wisconsin, 53706*

<sup>2</sup> *University and INFN of Pavia, Pavia, Italy*

<sup>3</sup> *University of Virginia, Charlottesville, Virginia, 22901*

<sup>4</sup> *University of California at Berkeley, Berkeley, California, 94720*

<sup>5</sup> *University of Pennsylvania, Philadelphia, Pennsylvania, 19104*

<sup>6</sup> *Northwestern University, Evanston, Illinois, 60208*

<sup>7</sup> *University of California at Los Angeles, Los Angeles, California, 90024*

<sup>8</sup> *Nanjing University, Nanjing, People's Republic of China*

<sup>9</sup> *University of South Alabama, Mobile, Alabama, 36688*

<sup>10</sup> *Vanier College, Montreal, Quebec, Canada*

<sup>11</sup> *University and INFN of Lecce, Lecce, Italy*

<sup>12</sup> *Duke University, Durham, North Carolina, 27706*

<sup>13</sup> *Prairie View A&M, Prairie View, Texas, 77446*

<sup>14</sup>*Shandong University, Jinan, Shandong, People's Republic of China*

<sup>15</sup>*University of Houston, Houston, Texas, 77204*

<sup>16</sup>*Fermilab, Batavia, Illinois, 60510*

<sup>17</sup>*Comenius University, Bratislava, Slovakia*

<sup>18</sup>*McGill University, Montreal, Quebec, Canada*

(March 26, 1997)

## Abstract

We present the  $x_F$  and  $p_T$  differential cross sections of  $J/\psi$  and  $\psi'$  respectively in the ranges  $-0.05 < x_F < 0.25$  and  $p_T < 3.5 \text{ GeV}/c$ . The data samples are constituted by about 12000  $J/\psi$  and 200  $\psi'$  produced in proton-silicon interactions at 800 GeV/c and decaying into opposite sign muons. The  $x_F$  and  $p_T$  distributions are compared with recent results from experiments E789 at the same energy and to leading order QCD predictions using the MRS D0 parametrization for the parton structure function. The measured shapes of the differential cross sections, except for the  $d\sigma/dx_F$  at small  $x_F$ , agree very well with the prediction, even though their value is quite larger. We also present the  $\cos\theta$  differential cross-section of the  $J/\psi$  which indicates unpolarized production in contrast with color octet models predictions [1,2].

## I. INTRODUCTION

Hadronic production of charmonium states is one of the most studied processes in high energy physics. In spite of this experimental effort, the mechanisms of quarkonium production are not well understood, and calculations of higher order contributions are still missing. In addition, the formation of the  $c\bar{c}$  bound states is a non-perturbative QCD process and requires some understanding of the evolution from the quark-antiquark color octet to the physical quarkonium states. The renewed interest in these subjects, owing to Tevatron collider results [3], has led to a better theoretical understanding of these mechanisms with the development of a new model in the past couple of years [1,2]. One of the feature of this new model is that it predicts high transverse polarization of quarkonium states.

The study of inclusive  $J/\psi$  production is complicated by additional contributions from radiative decays of higher-mass states ( $\chi_{i=0,1,2}$  and  $\psi'$ ) to the direct production, making comparison with theory more difficult. In this paper we report on the  $x_F$  and  $p_T$  differential cross sections for  $J/\psi$  and  $\psi'$  in the ranges  $-0.05 < x_F < 0.25$  and  $p_T < 3.5 \text{ GeV}/c$ . We compare these cross sections with the recent published results of experiment E789 [4] obtained at the same energy, and with leading order QCD calculations using MRS [5] parton distributions. We also report on measurement of the differential angular distribution of the  $J/\psi$  and compare this to the color octet predictions.

## II. EXPERIMENTAL SET-UP

### A. Beam and target

The data were collected at the High Intensity Laboratory in a primary proton beam at Fermilab with the E771 spectrometer during a short run of 5 weeks in December 1991.

The 800 GeV/c beam, of average intensity  $\approx 4 \times 10^7$  proton/s per 23s spill every 57s, interacted with a silicon target consisting of 12 foils, each 2 mm thick and spaced 4 mm apart, for a total of 5.3 % of an interaction length. The resulting average interaction rate was approximately 2 MHz.

The beam was monitored by means an ion chamber and beam silicon strip detectors placed along the beam line, which gave a total integrated number of live protons on target of  $1.313 \times 10^{13}$  with an error of approximately 5 % dominated by the uncertainty in the efficiency of the beam silicon detector.

## B. Spectrometer

The E771 spectrometer [6,7] was optimized for the observation of dimuons coming from  $J/\psi$ 's generated in the decays of heavy quark states. It consisted of a silicon microstrip detector, a tracking section upstream and downstream of an analysis magnet, an electromagnetic calorimeter and a muon detector placed after a hadron absorber. Neither the microstrip detector nor the calorimeter was used for the analysis described here.

The tracking section consisted of 22 planes of MWPC and 9 planes of drift chambers to define the charged particle trajectories upstream of the analysis magnet and of 12 planes of drift and 6 of drift-pad [8] chambers downstream of the magnet. All chambers are deadened in a region around the beam axis with a resulting minimum acceptance angle of 25 mrad. The analysis magnet, a dipole with  $185 \times 90$  cm<sup>2</sup> aperture, provided a  $p_T$  kick of 0.82 GeV/c in the horizontal plane.

The muon detector, located downstream of a 3 m thick hadron absorber, made of steel (copper in the central part), consisted of three planes of resistive plate counters (RPCs) and three planes of scintillators separated by steel, concrete and lead absorbers. The RPCs are thin gap (2 mm) gas devices operating in streamer mode under a high uniform electric field (40 kV/cm). The charge produced by the streamer process is picked up by external copper pads [9].

The single and dimuon triggers, entirely based on the RPC signals, define a muon as the triple coincidence among a projective set of pads belonging to the three RPC planes [10,11]. The minimum momentum required for a muon to penetrate the absorbers and produce a signal in the third RPC plane is 10 GeV/c in the central part and about 6 GeV/c at wider angles.

Further details of the E771 spectrometer can be found elsewhere [7].

### III. DATA ANALYSIS

The collected data amounted to about 130 million dimuon triggers and 60 million single muon triggers recorded on 1200 exabyte cassette tapes. The 130 million dimuon trigger events were processed with a fast filter program which, starting from muon candidates, defined as the coincidence of at least 4 out of the 3 RPC and 3 scintillator planes, reconstructed only the muon tracks downstream of the analysis magnet. In the subsequent analysis, these muons were fully tracked in all chambers and through the analysis magnet. Opposite sign dimuons, constrained to a common vertex, were selected. Only the pair with the best vertex constrained fit  $\chi^2$  was considered for this analysis.

The overall reconstruction efficiencies and acceptances were obtained by generating about  $10^6$  Monte Carlo (MC) events for the  $J/\psi$  and  $10^5$  for the  $\psi'$ . The first iteration differential distributions used in the MC were taken from earlier experiments at lower energy. The mesons were assumed to decay isotropically. The decay muons were propagated through a GEANT simulation of the E771 detector taking into account the measured chamber and trigger efficiencies [9–11] and the contribution of multiple scattering. To simulate realistic noise in the detector, the generated events were superimposed on real events. In the high end  $x_F$  bins the distribution of reconstructed masses was fit with two gaussians while the mass distribution on the midrange bins was fit with three gaussians. In the latter case the widest gaussians was considered as background because an independent study showed that events in the wider gaussian were primarily cases in which the reconstructed  $x_F$  was more than  $3\sigma$

different than the generated ones. The ranges of  $x_F$  and  $p_T$  over which the experiment is sensitive are respectively,  $-0.05 < x_F < 0.25$  and  $p_T < 3.5 \text{ GeV}/c$ . The average relative resolutions are 6.0 % in  $x_F$  and 6.7 % in  $p_T$ . The range for the angular distribution is  $-0.8 < \cos\theta < 0.8$ .

#### IV. EXPERIMENTAL RESULTS

Fig. 1 shows the invariant mass spectrum of the selected opposite sign di-muons. A total of  $11660 \pm 139 \text{ } J/\psi$  and  $218 \pm 24 \text{ } \psi'$  are obtained from fits to the background subtracted number of events in the two peaks. The dashed line represents the background, fitted to the function:

$$\frac{a}{m_{\mu\mu}^3} \exp(-bm_{\mu\mu}) , \quad (1)$$

which is mainly due to muons from  $\pi$  and  $K$  decays, to the Drell-Yan process and to charm production. Contributions from B mesons are negligible.

The mass resolution of the spectrometer depends on  $x_F$ , ranging from  $20 \text{ MeV}/c^2$  at  $x_F = -0.05$  to about  $100 \text{ MeV}/c^2$  at  $x_F = 0.25$ , while it is totally independent of the transverse momentum, in agreement with Monte Carlo simulation.

The differential distributions have been extracted by fitting the mass spectra in each of the  $x_F$  and  $p_T$  bins with the resolution functions of the two resonances (the sum of two gaussians for the  $J/\psi$  and a single gaussian for the  $\psi'$ ) over the described background. The use of two gaussians for the  $J/\psi$ , suggested by Monte Carlo studies, is motivated by the different quality of the information obtainable in highly populated hit regions.

In order to minimize systematics, the procedure for extracting the differential distribution was iterated by inserting into the Monte Carlo the extracted  $x_F$  and  $p_T$  distributions, corrected for the resulting acceptances and efficiencies, until convergence and stability of the result was reached.

The differential cross sections have been computed by assuming an atomic weight dependence  $A^\alpha$ , with  $\alpha = 0.920 \pm 0.008$  [12]. The choice of this value is justified by the adequate

description of the available data [12] for a silicon target ( $A=28$ ) and, because in our range of  $x_F$  and  $p_T$ ,  $\alpha$  appears to be fairly constant [12,13]. The values of the branching ratios  $BR(J/\psi \rightarrow \mu^+\mu^-)$  and  $BR(\psi' \rightarrow \mu^+\mu^-)$  have been taken from Ref. [14].

The measured differential cross sections for each of the  $x_F$  and  $p_T$  bins are listed in Table I for the  $J/\psi$  and in Table II for the  $\psi'$ . In addition to the errors shown there are overall systematic uncertainties of 8 % for the  $J/\psi$  and 23 % for the  $\psi'$ , due to the uncertainties in luminosity, branching ratios and acceptance.

The  $d\sigma/dx_F$  cross sections per nucleon are shown in Fig. 2 as a function of the fractional longitudinal momentum  $x_F$  of the  $J/\psi$  and  $\psi'$ . The data have been fit with an empirical function of the form

$$\frac{d\sigma}{dx_F} = A(1 - |x_F|)^n \quad (2)$$

The fit parameters are shown in Table III. The first row in the table shows the results of a fit to all the data points, while the second row (corresponding to the line fit of Fig. 2) shows the fit excluding the two negative  $x_F$  values. The fourth row in Tab. III lists the fit parameters for  $\psi'$  when  $n$  is forced to be equal to the corresponding value of the  $J/\psi$  fit.

Analogously, the  $d\sigma/dp_T^2$  cross sections per nucleon versus the transverse momentum of the produced meson, for both charmonium states, are shown in Fig. 3. The data were parametrized by:

$$\frac{d\sigma}{dp_T^2} = A \exp(-np_T^2) \quad (3)$$

Again, the fit parameters are listed in Table III. The fifth row in the table shows the results of a fit to all data points. The fit for the  $J/\psi$  has been also performed by excluding the last two points in order to directly compare our result to the one of FNAL E789 [4] where a smaller range of  $p_T$  is used. The parameters of this fit are listed in the sixth row of Table III.

It is worth noticing that, within experimental errors, both differential cross sections for the two charmonium states are described by the same parameters, suggesting that they are

produced by the same mechanisms. In fact, Fig. 4 shows that there is no evident dependence on  $x_F$  and  $p_T$  of the ratio:

$$\frac{BR(\psi' \rightarrow \mu^+ \mu^-) \sigma(\psi')}{BR(J/\psi \rightarrow \mu^+ \mu^-) \sigma(J/\psi)} \quad (4)$$

in which the uncertainties in the absolute normalization and the systematics arising from the knowledge of the branching ratios cancel out. These results seem to disagree with recently published data at same energy [4] where a mild increase in this ratio with  $x_F$  and  $p_T$  is reported.

In Fig. 5 and Fig. 6 we compare our  $x_F$  and  $p_T$  distributions for the  $J/\psi$  and  $\psi'$  with those of Fermilab E789 [4]. The cross sections of the two experiments differ by an overall scale factor because of a different choice of the parameter  $\alpha$  (E789 uses  $\alpha = 0.9$ , instead of  $\alpha = 0.92$  which gives a difference of about 11 % for the E789 target with  $A=197$ ).

While the shapes of  $d\sigma/dp_T^2$  are in very good agreement, the  $x_F$  distributions show some discrepancy ( $n_{E789} = 4.91 \pm 0.18$ ,  $n_{E771} = 6.38 \pm 0.24$ ). The nature of this inconsistency is unknown. It could perhaps be attributed to nuclear effects of the structure functions, because of the large difference in the atomic weights of the targets ( $A_{E789} = 197$  instead of  $A_{E771} = 28$ ).

In Fig. 5 and Fig. 6 we compare also our results to the theoretical predictions [15] computed using perturbative QCD to leading order for both differential distributions of the two charmonium states. These predictions are still based the on Color Singlet Model [16], because the differential distribution for the most advanced model developed in the last years, the Color Octet Mechanism [1], are not yet available at low  $p_T$ . The contributions of various quarkonium states to the inclusive  $J/\psi$  cross section are taken into account by using the known branching ratio of the  $\chi_{0,1,2}$  and  $\psi'$  states decaying in  $J/\psi$  [14]. The Martin-Roberts-Stirling set D0 (MRS D0) [5] for the parton structure function has been used for comparison with our data.

Both the shapes and the scale of the theoretical predictions disagree with our data for the  $d\sigma/dx_F$  cross sections. The  $K$  factors needed to normalize the curves are  $K \approx 4$  for  $J/\psi$

and  $K \approx 16$  for  $\psi'$  while the disagreement in shape is mainly at small  $x_F$ .

The shape of  $d\sigma/dp_T^2$  cross sections is in good agreement with our data, but still needs a scale factor for the normalization. In this case  $K \approx 9$  for  $J/\psi$ , while for  $\psi'$   $K \approx 14$  needs to be used. These  $d\sigma/dp_T^2$  predictions are obtained by assuming an intrinsic  $p_T$  gaussian distribution for the partons with  $\langle p_T^2 \rangle = 0.5 (GeV/c)^2$ . To eliminate the divergences at low  $p_T$  due to  $\chi_0$  and  $\chi_2$  states we had to apply an arbitrary cutoff at  $0.6 GeV/c$  for the  $J/\psi$  and at  $0.4 GeV/c$  for the  $\psi'$ . In fact, the listed  $K$  factors depends strongly on the choice of this cut and therefore are experiment dependent.

We also computed the total cross sections for  $J/\psi$  and  $\psi'$ . Assuming that equation 2 describes all the  $x_F$  range, we get  $\sigma(J/\psi) = 375 \pm 4 \pm 30 nb$  and  $\sigma(\psi') = 46 \pm 3 \pm 10 nb$ . These values are consistent with those obtained in a previous analysis [17] and with a recent computation of the total cross-section using the Color Octet Model [2].

Finally the same procedure was used to obtain the  $d\sigma/d\cos\theta$  differential cross-section shown in Fig. 7. The angle  $\theta$  is defined as the angle between the positive muon and beam direction in the  $J/\psi$  rest frame. In this case the fit has been performed with the function  $A(1 + \alpha\cos^2\theta)$  obtaining  $\alpha = -0.09 \pm 0.12$ . This result is in disagreement with the color octet model [2] which predicts a sizeable  $J/\psi$  transverse polarization, emphasizing the need for the inclusion of higher twist terms in the description of quarkonium production.

## ACKNOWLEDGEMENTS

We thank M.L.Mangano for his support and the discussions about the QCD theoretical distributions. We acknowledge the invaluable help of the Fermilab staff including the Research and Computing Division personnel. This work is supported by the U.S. Department of Energy, the National Science Foundation, the Natural Science and Engineering Research Council of Canada, the Istituto Nazionale di Fisica Nucleare of Italy and the Texas Advanced Research Program.

## REFERENCES

- [1] E.Braaten and S.Fleming Phys. Rev. Lett. **74**, 3327 (1995),  
P.Cho and A.K.Leibovich, Phys. Rev. D **53**, 150 (1996).
- [2] M.Beneke and I.Z. Rothstein, SLAC-Pub-7129, March 1996.
- [3] CDF Collaboration, F.Abe *et al.*, Fermilab-Conf-94/136,  
F.Abe *et al.*, Fermilab-Conf-95/128.
- [4] M.H. Schub *et al.*, Phys. Rev. D **52**, 1307 (1995).
- [5] A.D. Martin, W.J. Stirling and R.G. Roberts, Phys. Lett B **306**, 145 (1993).
- [6] T. Alexopoulos *et al.*, Nucl. Phys. B **27**, 257 (1992).
- [7] T. Alexopoulos *et al.*, to be published in Nucl. Instr. and Meth. A **376**, issue 3, July  
11th 1996.
- [8] L. Spiegel *et al.*, FERMILAB-TM-1765 (1991).
- [9] G. Cataldi *et al.*, Nucl. Instr. and Meth. A **337**, 350 (1994).
- [10] L. Antoniazzi *et al.*, Nucl. Instr. and Meth. A **355**, 320 (1995).
- [11] L. Antoniazzi *et al.*, Nucl. Instr. and Meth. A **360**, 334 (1995).
- [12] M.R. Adams *et al.*, Phys. Rev. Lett. **66**, 133 (1991).
- [13] M.J. Leitch *et al.*, Phys. Rev. D **52**, 4251 (1995).
- [14] Review of Particle Properties 1994, Phys. Rev. D **50**, 1173 (1994).
- [15] M.L. Mangano (private communication), Quarkonium Productions Codes (unpub-  
lished).
- [16] E.L.Berger and D.Jones, Phys Rev. D **23**, 1521 (1981),  
B.Guberina *et al.*, Nucl. Phys. B **174**, 317 (1981),

R.Bayer and R.Rückl, Z. Phys. C **19**, 251 (1983),

B.Humbert, Phys. Lett. B **184**, 105 (1987),

R.Gastmans *et al.*, Nucl. Phys. B **291**, 731 (1987).

[17] T.Alexopoulos *et al.*, Phys. Lett. B **374**, 271 (1996).

TABLES

TABLE I.  $J/\psi$  cross section for each bin of  $x_F$  and  $p_T$ . There is an overall systematic error of 8 %.

$x_F$ bin	$d\sigma/dx_F$ [nb/nucleon]	$p_T$ bin [GeV/c]	$d\sigma/dp_T^2$ [nb(GeV/c) <sup>-2</sup> /nucleon]
-0.05 ÷ -0.03	1309 ± 78	0.0 ÷ 0.3	197 ± 17
-0.03 ÷ -0.01	1352 ± 70	0.3 ÷ 0.6	175.9 ± 9.8
-0.01 ÷ 0.01	1327 ± 56	0.6 ÷ 0.9	134.9 ± 5.9
0.01 ÷ 0.03	1242 ± 48	0.9 ÷ 1.2	101.1 ± 4.2
0.03 ÷ 0.05	1134 ± 44	1.2 ÷ 1.5	64.7 ± 2.8
0.05 ÷ 0.07	963 ± 46	1.5 ÷ 1.8	41.5 ± 2.3
0.07 ÷ 0.09	776 ± 35	1.8 ÷ 2.1	22.6 ± 1.6
0.09 ÷ 0.11	701 ± 36	2.1 ÷ 2.4	12.3 ± 1.4
0.11 ÷ 0.13	591 ± 35	2.4 ÷ 2.8	4.8 ± 0.5
0.13 ÷ 0.15	508 ± 34	2.8 ÷ 3.2	1.84 ± 0.27
0.15 ÷ 0.17	463 ± 39	3.2 ÷ 3.6	0.59 ± 0.20
0.17 ÷ 0.19	427 ± 38		
0.19 ÷ 0.21	353 ± 40		
0.21 ÷ 0.23	254 ± 28		
0.23 ÷ 0.25	294 ± 39		

TABLE II.  $\psi'$  cross section for each bin of  $x_F$  and  $p_T$ . There is an overall systematic error of 23 %.

$x_F$ bin	$d\sigma/dx_F$ [nb/nucleon]	$p_T$ bin [GeV/c]	$d\sigma/dp_T^2$ [nb(GeV/c) <sup>-2</sup> /nucleon]
-0.06 ÷ -0.02	148 ± 59	0.0 ÷ 0.4	25.1 ± 8.0
-0.02 ÷ 0.02	199 ± 45	0.4 ÷ 0.7	23.3 ± 5.4
0.02 ÷ 0.06	127 ± 30	0.7 ÷ 1.0	15.3 ± 4.0
0.06 ÷ 0.10	82 ± 25	1.0 ÷ 1.4	13.6 ± 2.2
0.10 ÷ 0.14	87 ± 18	1.4 ÷ 2.4	2.4 ± 0.7
0.14 ÷ 0.18	54 ± 12	2.4 ÷ 3.4	0.51 ± 0.26
0.18 ÷ 0.22	37 ± 17		
0.22 ÷ 0.26	32 ± 13		

TABLE III. Results of the fits performed on the differential distributions as described in the text.

meson	function	$A$	$n$	$\chi^2/DOF$
$J/\psi$	$A(1 -  x_F )^n$	$1424 \pm 31 \text{ nb}$	$6.54 \pm .23$	1.65
$J/\psi$	$A(1 -  x_F )^n$	$1386 \pm 33 \text{ nb}$	$6.38 \pm .24$	0.92
$\psi'$	$A(1 -  x_F )^n$	$178 \pm 29 \text{ nb}$	$6.7 \pm 1.3$	0.24
$\psi'$	$A(1 -  x_F )^n$	$172 \pm 17 \text{ nb}$	6.38( <i>fixed</i> )	0.26
$J/\psi$	$A \exp(-np_T^2)$	$182 \pm 5 \text{ nb}(\text{GeV}/c)^{-2}$	$0.54 \pm 0.01 (\text{GeV}/c)^{-2}$	0.93
$J/\psi$	$A \exp(-np_T^2)$	$185 \pm 5 \text{ nb}(\text{GeV}/c)^{-2}$	$0.55 \pm 0.01 (\text{GeV}/c)^{-2}$	0.60
$\psi'$	$A \exp(-np_T^2)$	$27 \pm 4 \text{ nb}(\text{GeV}/c)^{-2}$	$0.61 \pm 0.08 (\text{GeV}/c)^{-2}$	1.02

# FIGURES

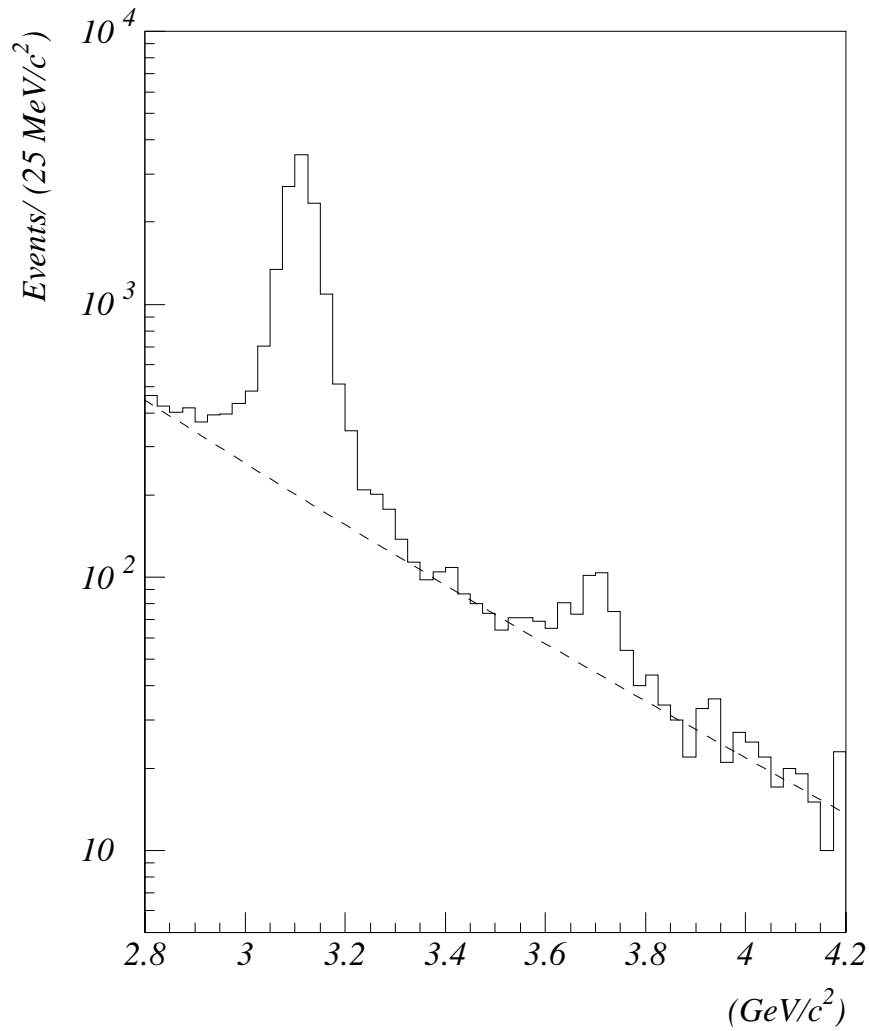


FIG. 1. Invariant mass spectrum of the  $\mu^+\mu^-$  pairs. The dashed line is the continuum background as described in the text.

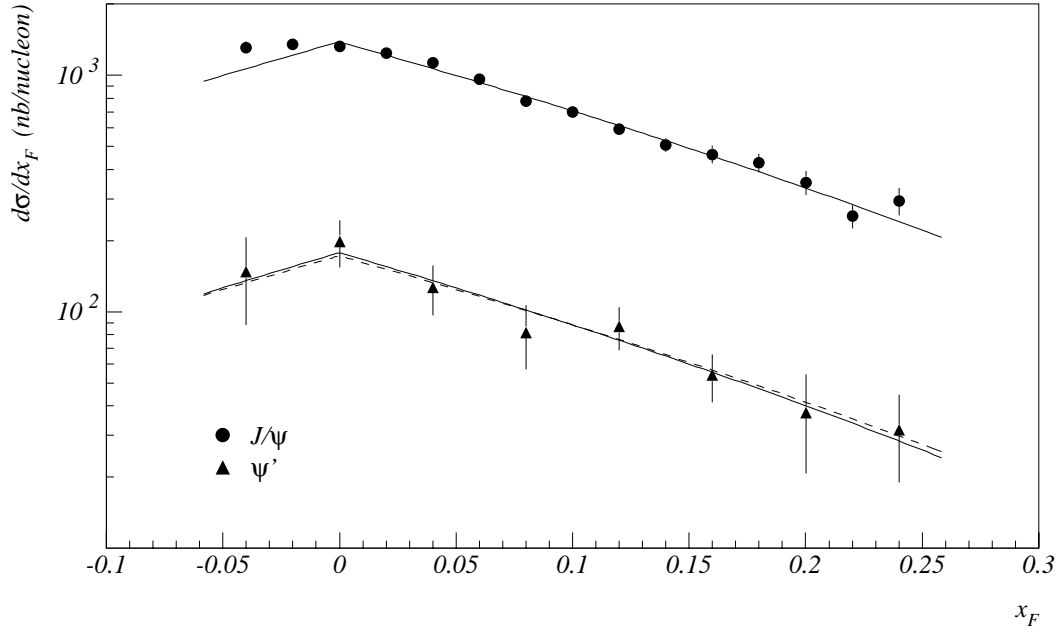


FIG. 2. Differential cross sections for  $J/\psi$  and  $\psi'$  versus  $x_F$ . The 8 % ( $J/\psi$ ) and 23 % ( $\psi'$ ) systematic uncertainties due to the normalization are not shown. Superimposed on the data are the fits described in the text. The dashed line is a fit to the  $\psi'$  data with the exponential parameter fixed to the corresponding value for  $J/\psi$ .

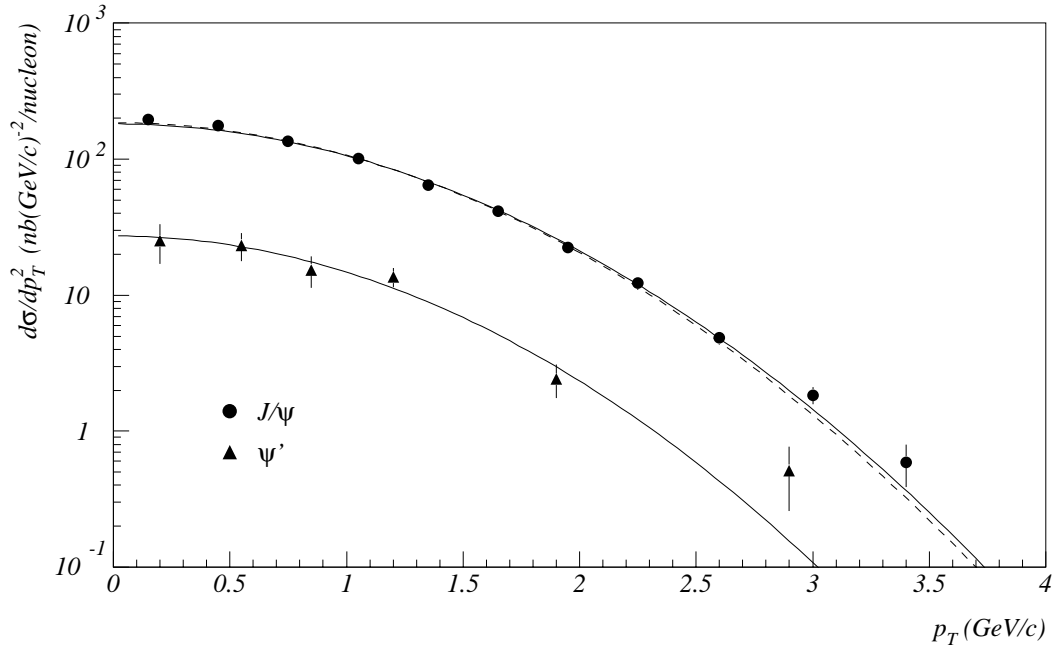


FIG. 3. Differential cross sections for  $J/\psi$  and  $\psi'$  versus  $p_T$ . The 8 % ( $J/\psi$ ) and 23 % ( $\psi'$ ) systematic uncertainties due to the normalization are not shown. Superimposed on the data are the fits described in the text. The dashed line is a fit to the  $J/\psi$  data performed by excluding the last two points.

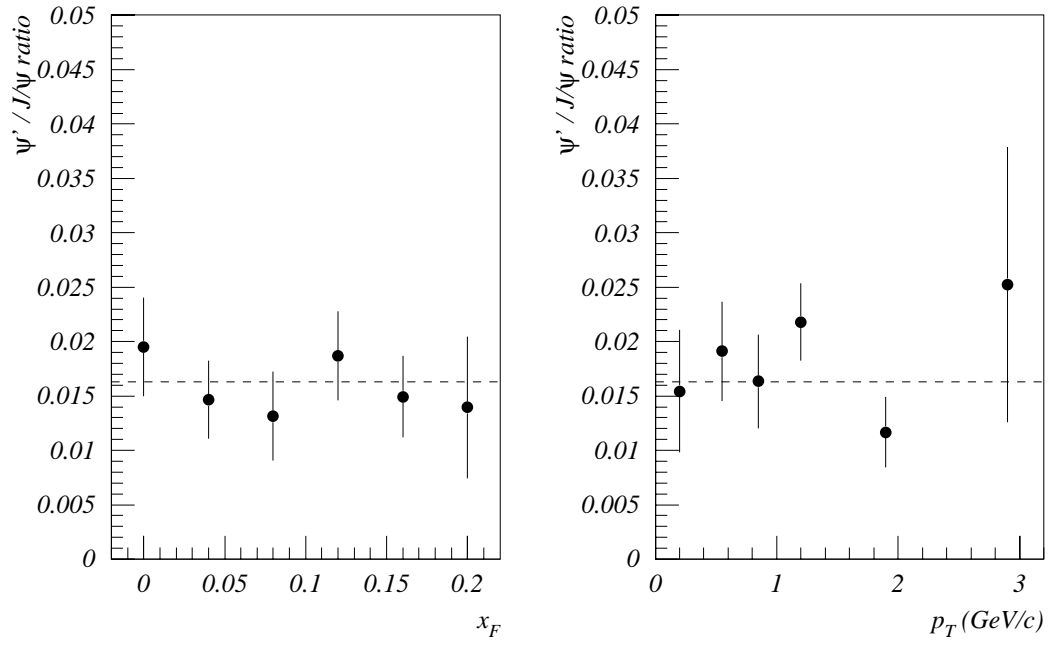


FIG. 4. Ratio  $BR(\psi' \rightarrow \mu^+ \mu^-) \times \sigma(\psi')$  to  $BR(J/\psi \rightarrow \mu^+ \mu^-) \times \sigma(J/\psi)$  versus  $x_F$  and  $p_T$ .

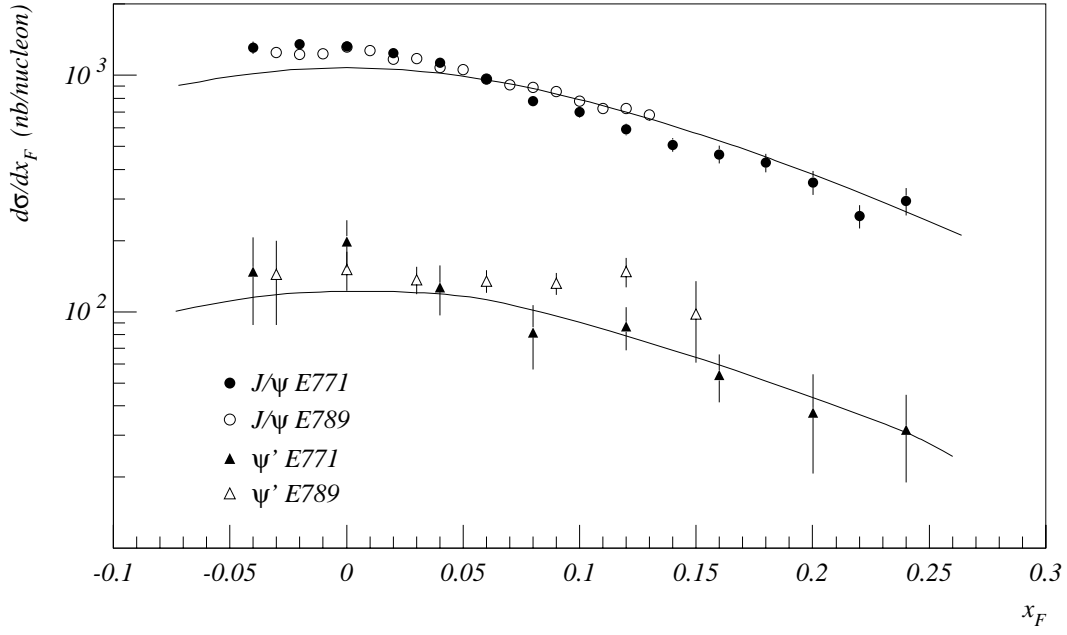


FIG. 5. E771 differential cross sections for  $J/\psi$  and  $\psi'$  versus  $x_F$  compared with the E789 results and with MRSD0 theoretical predictions, arbitrarily normalized to E771 data.

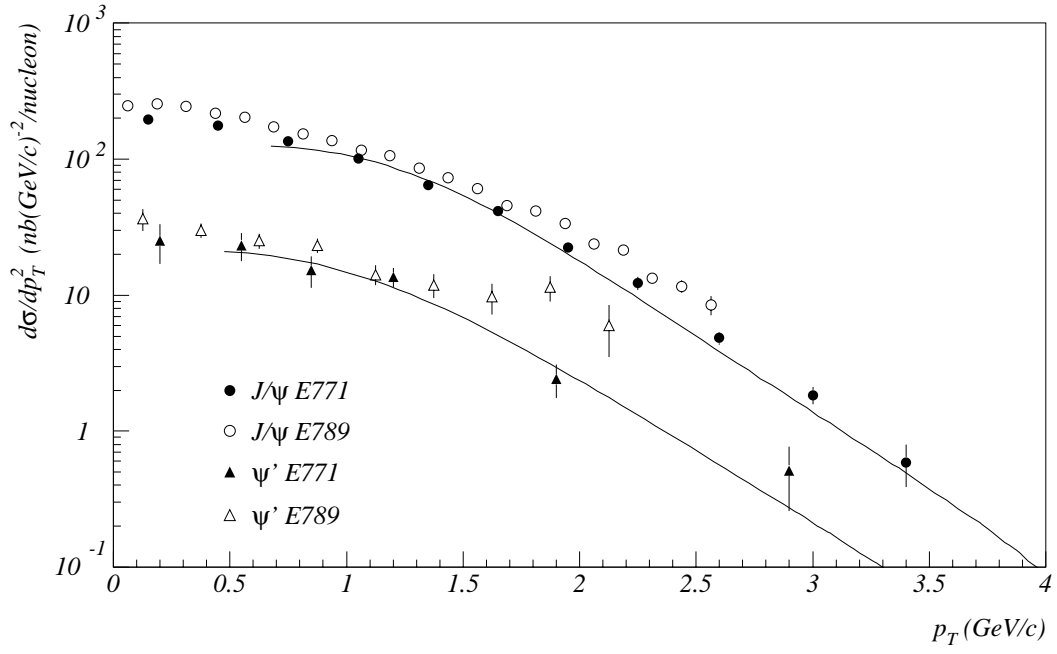


FIG. 6. E771 differential cross sections versus  $p_T$  compared with the E789 results and with MRSD0 theoretical predictions, arbitrarily normalized to E771 data.

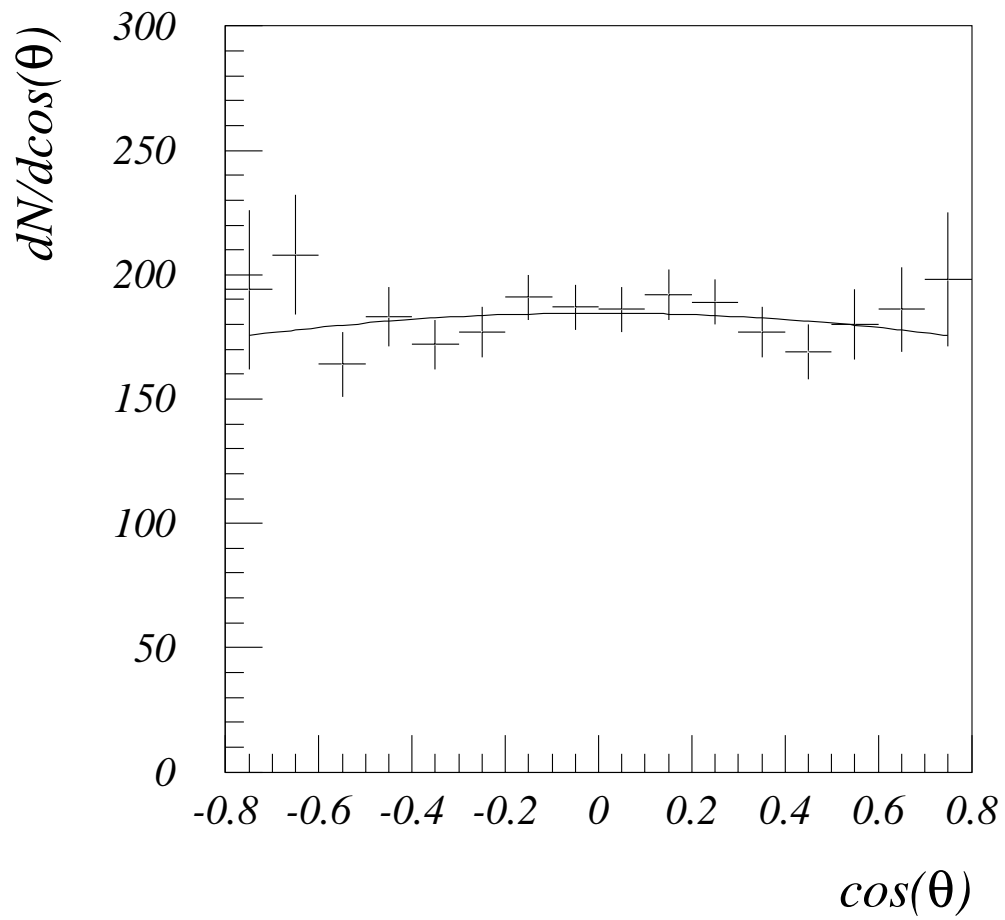


FIG. 7.  $\cos\theta$  differential cross section. Superimposed on the data is the fit described in the text.